

Single impurities in a Bose-Einstein condensate can make two polaron flavors

A. A. Blinova^{1,2}, M. G. Boshier¹, and Eddy Timmermans³

¹*P-21, Physics Division, Los Alamos National Laboratory, Los Alamos, New Mexico 87545*

²*Physics & Astronomy Department, Rice University, Houston, Texas 77251 and*

³*T-4, Theory Division, Los Alamos National Laboratory, Los Alamos, New Mexico 87545*

Polarons, self-localized composite objects formed by the interaction of a single impurity particle with a host medium, are a paradigm of strong interaction many-body physics. We show that dilute gas Bose-Einstein condensates (BEC's) are the first medium known to self-localize the same impurity particles both in a Landau-Pekar polaron state akin to that of self-localized electrons in a dielectric lattice, and in a bubble state akin to that of electron bubbles in helium. We also show that the BEC-impurity system is fully characterized by just two dimensionless coupling constants, and that it can be adiabatically steered from the Landau-Pekar regime to the bubble regime in a smooth crossover trajectory.

PACS numbers: 05.30.Jp, 03.75.Hh, 67.85.Hj, 67.85.Bc

The polaron, a single distinguishable particle that interacts with the self-consistent deformation of the medium that contains it, is a paradigm of strong interaction physics in condensed matter [1, 2], chemistry [3], and biophysics [4]. Polarons self-localize when sufficiently cold and strongly coupled to the host medium. In nature, large [5] polarons appear in two flavors: particles that hardly deform the medium, such as electrons in dielectric lattices [6], and particles that greatly distort the medium, such as electron bubbles in condensed helium superfluids [7]. In the first class, the particle is accompanied by a cloud of small amplitude collective excitations of the medium which, as first shown by Landau and Pekar [8, 9], can be integrated out in the strong coupling limit. In the bubble systems, which occur in fluids and dense gases, Kuper [10] showed that the strongly repelling particle can be described as residing in a self-created cavity – the “bubble” – surrounded by the fluid. The effective mass and mobility of bubble and Landau-Pekar polarons exhibit quite different behaviors, and so the two polaron flavors are customarily treated as distinct. However, as we show below, dilute gas Bose-Einstein condensates (BECs) [11, 12], unlike previously known host media, can self-localize neutral impurity atoms [13, 14] in both the bubble and Landau-Pekar polaron states. Further, the system phase diagram presented here shows how the strongly coupled BEC-impurity polaron evolves continuously between these limits as the interaction strengths and BEC density are varied. The BEC-impurity system can therefore be regarded as a quantum simulator of large polarons in a boson environment [15], complementing recent proposals for simulating lattice polarons [16–19].

The system: We consider a neutral impurity atom of mass m_I immersed in a homogeneous BEC of N boson particles of mass m_B contained in a macroscopic volume Ω , giving an average density $\rho = N/\Omega$. Bosons at positions \mathbf{r} and \mathbf{r}' interact via a repulsive short-range interaction of scattering length a_{BB} , described by an effective potential $V_{BB}(\mathbf{r} - \mathbf{r}') = \lambda_{BB}\delta(\mathbf{r} - \mathbf{r}')$, where $\lambda_{BB} = (4\pi\hbar^2/m_B)a_{BB}$ and $a_{BB} > 0$. The boson chemical potential $\mu_B = \lambda_{BB}\rho$ sets the time scale \hbar/μ_B and the

coherence length $\xi = 1/\sqrt{16\pi\rho a_{BB}}$ sets the length scale on which the BEC can respond to a perturbation. The perturbation here is provided by the impurity interacting with the bosons via $V_{IB}(\mathbf{r} - \mathbf{x}) = \lambda_{IB}\delta(\mathbf{r} - \mathbf{x})$, where \mathbf{x} represents the impurity position and the impurity-boson interaction strength $\lambda_{IB} = 2\pi\hbar^2(m_I^{-1} + m_B^{-1})a_{IB}$ is proportional to the impurity-boson scattering length a_{IB} , taken to be Feshbach-tuned [20] to a large positive value [21]. We break the translational symmetry of the BEC-impurity system ground state by fixing the impurity center-of-mass position at $\mathbf{r} = 0$ [22]. We write the BEC density in the presence of the impurity as $\rho_B(\mathbf{r}) = \rho + \delta\rho_B(\mathbf{r})$. Self-localization occurs when the effective potential $\lambda_{IB}\delta\rho_B(\mathbf{r})$ can trap the impurity. We classify $|\delta\rho_B(\mathbf{r} = 0)/\rho| < 0.1$ as the Landau-Pekar regime [13], and $|\delta\rho_B(\mathbf{r} = 0)/\rho| > 0.9$ as the bubble regime. We will show that in these regimes the impurity observables exhibit the scaling behaviors expected from the simplified Landau-Pekar and bubble descriptions respectively.

Landau-Pekar polaron: The impurity-boson repulsion can be simultaneously strong enough to self-trap the impurity, and weak enough to hardly change the BEC density profile [Fig. 1(a)]. In this regime, the Bogoliubov expansion and transformation that describes the BEC fluctuations [23] can be carried out around the homogeneous BEC [24]. The interaction of the dilute BEC with an impurity of density $\rho_I(\mathbf{r}) = (2\pi)^{-3} \int d^3\mathbf{k} e^{i\mathbf{k}\cdot\mathbf{r}} \rho_{I,\mathbf{k}}$ then gives a Fröhlich hamiltonian [25], familiar from electron-phonon interactions. Representing the quasi-particle annihilation/creation operators of momentum \mathbf{k} and energy $\hbar\omega_{\mathbf{k}} = \hbar k\sqrt{(1 + \xi^2 k^2)(\mu_B/m_B)}$ by $b_{\mathbf{k}}, b_{\mathbf{k}}^\dagger$, the impurity-boson interaction is described by

$$H_{IB} = \frac{\lambda_{IB}}{\Omega} \sum_{\mathbf{k}} \rho_{I,-\mathbf{k}} \rho_{B,\mathbf{k}} \approx \lambda_{IB}\rho + \frac{M}{\sqrt{\Omega}} \sum_{\mathbf{k}} \nu_{\mathbf{k}} \rho_{I,-\mathbf{k}} (b_{\mathbf{k}}^\dagger + b_{\mathbf{k}}), \quad (1)$$

where $\rho_{B,\mathbf{k}}$ is the operator associated with the boson density. In Eq. (1), the impurity-phonon interaction matrix

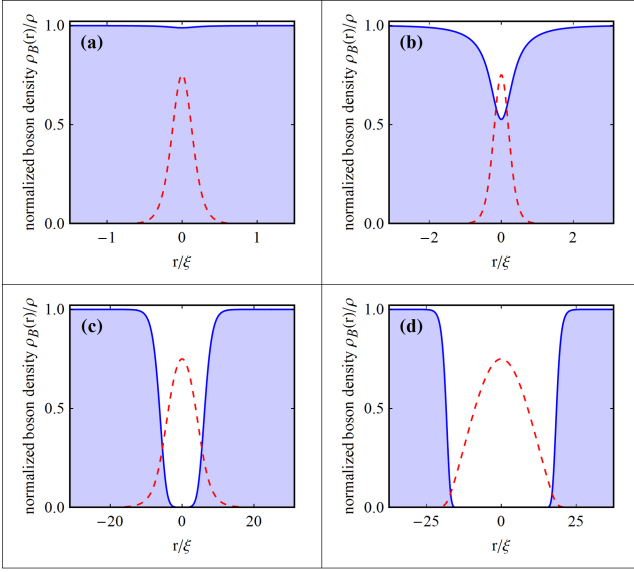


FIG. 1: Numerical results for the normalized boson density (blue shading) and un-normalized impurity wavefunction (red dashed line). Parameter values [see Eqs. (3) and (8)]: (a) $\beta = 25$ and $\alpha = 10^{-9}$, (b) $\beta = 25$ and $\alpha = 10^{-5}$, (c) $\beta = 25$ and $\alpha = 10^1$, (d) $\beta = 5 \times 10^4$ and $\alpha = 10^3$.

element $M = \lambda_{IB}\sqrt{\rho}$, and $\nu_{\mathbf{k}} = (\xi^2 k^2 / [1 + \xi^2 k^2])^{1/4}$ is a structure factor arising from the Bogoliubov transformation. By showing that the Fröhlich coupling H_{IB} amounts to a displacement of the \mathbf{k} -mode oscillator coordinate $\phi_{\mathbf{k}} = (b_{\mathbf{k}}^\dagger + b_{-\mathbf{k}}) / \sqrt{2}$, Landau and Pekar [9] integrated out the phonon modes. The resulting energy reduction takes the form of a self-interaction [24, 26], $\Delta E = -M^2 (2\pi)^{-3} \int d^3\mathbf{k} \rho_{I,-\mathbf{k}} \rho_{I,\mathbf{k}} (\nu_{\mathbf{k}}^2 / \hbar\omega_{\mathbf{k}})$, which in the strongly coupled regime overcomes the kinetic energy cost of localizing the impurity. Here, the self-interaction potential is an attractive Yukawa potential of range ξ . It can cause self-localization when ξ exceeds the impurity extent, which is comparable to [13]

$$R_o = [4\pi\rho a_{IB}^2 (1 + m_I/m_B) (1 + m_B/m_I)]^{-1}. \quad (2)$$

Specifically, when the ratio of the boson healing length ξ to the self-localization length R_o

$$\beta = \frac{\xi}{R_o} = \sqrt{\pi\rho} \frac{a_{IB}^4}{a_{BB}} \left(1 + \frac{m_I}{m_B}\right) \left(1 + \frac{m_B}{m_I}\right) \geq 5, \quad (3)$$

the above description predicts self-localization [13]. Note that the impurity extent $R_o = \xi/\beta$ can be significantly smaller than ξ , making this polaron a sub-coherence length structure. The binding energy, proportional to

$$E_o = \frac{\hbar^2}{2m_I R_o^2} = 2 \left(\frac{m_B}{m_I}\right) \beta^2 \mu_B, \quad (4)$$

then significantly exceeds μ_B . When scaled by E_o and R_o , impurity observables in the Landau-Pekar regime depend only on the dimensionless coupling strength β [13].

Bubble polaron: When a_{IB} grows sufficiently to expel the BEC from the impurity's vicinity [Fig. 1(c) and (d)], a Bogoliubov procedure should expand around the deformed BEC. However, a bubble description such as Kuper's model of electron bubbles in helium is a simpler starting point [10]. With complete BEC and impurity separation [Fig. 1(d)] the impurity, trapped in a self-created spherical cavity of radius R_c and volume V_c , has wavefunction $\chi(r) = \sqrt{\pi R_c^{-1}} \sin(\pi r/R_c)/r$. Neglecting surface tension, the system energy difference E_c with and without impurity is the impurity kinetic energy $\pi^2 \hbar^2 / (m_I R_c^2)$ plus the energy cost of making the cavity, PV_c , where $P = \lambda_{BB}\rho^2/2$ is the BEC pressure. Hence

$$E_c(R_c) = \frac{\pi^2 \hbar^2}{m_I R_c^2} + \frac{8\pi^2}{3} \frac{\hbar^2 a_{BB}}{m_B} \rho^2 R_c^3. \quad (5)$$

The minimization $\partial E_c / \partial R_c = 0$ yields the expected cavity radius $R_c = [4(m_I/m_B)\rho^2 a_{BB}]^{-1/5}$, and the impurity energy $E_c = (5/3)(\pi^2 \hbar^2 / [m_I R_c^2]) = (5\pi/2^{11/5})(m_B/m_I)^{3/5} \mu_B / [\sqrt{\rho a_{BB}^3}]^{2/5}$.

BEC permeability: The radical change in BEC-impurity overlap seen in Fig. 1(a) - (d) is due to a BEC “stiffness” arising because it costs kinetic and interaction energy to move $\Delta N_B = |\int d^3\mathbf{r} [\rho_B(\mathbf{r}) - \rho]|$ bosons away from the impurity. Estimating the interaction energy cost as $E_x = \Delta N_B \mu_B$ and using the predicted displaced boson number from [27], $\Delta N_B = |\lambda_{IB}/\lambda_{BB}|$ (valid in the Landau-Pekar and crossover regimes but not in the bubble regime), gives $E_x = |\lambda_{IB}/\lambda_{BB}| \mu_B$. The ratio

$$\sigma = \frac{E_x}{E_o} = \left[4\pi\rho a_{IB}^3 \left(1 + \frac{m_I}{m_B}\right)^3 \left(\frac{m_B}{m_I}\right)^2\right]^{-1} \quad (6)$$

then quantifies the relative importance of the displacement energy cost to the overlap energy gain of self-localization. We refer to σ as the BEC-impurity “permeability”. In the Landau-Pekar regime, a direct analytical evaluation yields $|\delta\rho_B(\mathbf{r}=0)/\rho| = (4\sqrt{2}/3\sqrt{\pi})\sigma^{-1} = 1.064\sigma^{-1}$. Thus, $\sigma \gg 1$ implies Landau-Pekar conditions where the repulsion is insufficient to overcome the BEC stiffness and displace the bosons noticeably [Fig. 1(a)]. A gradual increase in a_{IB} then expels the bosons significantly when $\sigma \sim 1$ [Fig. 1(b)], and enters the large-depletion bubble limit [Fig. 1(c) and (d)] when $\sigma \ll 1$.

General case: A more general ground state treatment, encompassing the Landau-Pekar and bubble regimes as limits, is based on the strong coupling approximation of a many-body product state. Minimizing the energy while requiring the respective boson and impurity wavefunctions $\psi(\mathbf{r})$ and $\chi(\mathbf{r})$ to be normalized gives two coupled Gross-Pitaevskii equations

$$\begin{aligned} \mu_B \psi(\mathbf{r}) &= -\frac{\hbar^2 \nabla^2}{2m_B} \psi(\mathbf{r}) + \lambda_{BB} |\psi(\mathbf{r})|^2 \psi(\mathbf{r}) \\ &\quad + \lambda_{IB} |\chi(\mathbf{r})|^2 \psi(\mathbf{r}) \\ \epsilon_I \chi(\mathbf{r}) &= -\frac{\hbar^2 \nabla^2}{2m_I} \chi(\mathbf{r}) + \lambda_{IB} |\psi(\mathbf{r})|^2 \chi(\mathbf{r}), \end{aligned} \quad (7)$$

where $\lim_{r \rightarrow \infty} \psi(r) = \sqrt{\rho}$, and μ_B and ϵ_I represent the Lagrange multipliers ensuring normalization, $\int d^3\mathbf{r} |\psi(\mathbf{r})|^2 = N$, $\int d^3\mathbf{r} |\chi(\mathbf{r})|^2 = 1$.

The BEC-impurity system has five physical parameters – m_B, m_I, ρ, a_{BB} and a_{IB} – but we find that the proper dimensional scaling of energies, density, and distances reveals a minimal dependence on just two coupling constants. The first is the length scale ratio $\beta = \xi/R_o$. The second is the mass-scaled boson gas parameter

$$\alpha = \left(\frac{m_B}{m_I} \right) \sqrt{\rho a_{BB}^3}. \quad (8)$$

All properly scaled observables can be cast in terms of α and β . For example, the permeability parameter σ takes the form $\sigma(\alpha, \beta) = 1/(4\pi^{1/4} \sqrt{\alpha\beta^3})$, and in the bubble limit the energy and cavity radius are given by $E_c = E_o (5\pi/24) \beta^2 (4/\alpha)^{2/5}$ and $R_c = R_o 4\pi^{1/2} \beta \alpha^{1/5}$, respectively. To prove the minimal dependence, we substitute (real-valued) scaled dimensionless boson (p) and impurity (g) wavefunctions:

$$\begin{aligned} \psi(\mathbf{r}) &= \sqrt{\rho} p(\mathbf{x} = \mathbf{r}/\xi) \\ \chi(\mathbf{r}) &= R_o^{-3/2} g(\mathbf{y} = \mathbf{r}/R_o), \end{aligned} \quad (9)$$

into the coupled equations (7), scaling the energies and lengths to obtain the dimensionless form

$$\begin{aligned} \left(\nabla_x^2 + \frac{1-p^2(\mathbf{x})}{2} \right) p(\mathbf{x}) &= -\frac{4\pi\beta^2}{\sigma(\alpha, \beta)} g^2(\mathbf{y} = \mathbf{x}\beta) p(\mathbf{x}) \\ (\nabla_y^2 + e_I) g(\mathbf{y}) &= -\sigma(\alpha, \beta) p^2(\mathbf{x} = \mathbf{y}/\beta) g(\mathbf{y}), \end{aligned} \quad (10)$$

where $e_I = \epsilon_I/E_o$, and the g, p solutions have to satisfy the normalization $\int d^3\mathbf{y} g^2(\mathbf{y}) = 1$ and boundary condition $\lim_{x \rightarrow \infty} p(\mathbf{x}) = 1$. Since the scaled coupled equations depend only on α and β [28] the BEC-impurity phase diagram is two-dimensional (2D).

Numerical solutions of the coupled equations (7) provide a rigorous test of the Landau-Pekar and bubble limiting behaviors by determining the α - and β -dependences of the relevant observables. For example, in Fig. 2 we plot the root mean-square impurity extent $R_{rms} = \sqrt{\int d^3\mathbf{r} r^2 \rho_I(\mathbf{r})}$. Each curve shows R_{rms}/R_o as a function of α for a specific β -value on a log-log plot, with arrows indicating α values corresponding to unit permeability $\sigma = 1$. On the left, the α -independence of the Landau-Pekar impurity properties is confirmed by the zero slope of the curves, which also show the expected convergence to $R_{rms} \approx 4.6 R_o$ for $\beta \geq 20$ [13]. On the right, the straight lines of slope $1/5$ confirm the expected bubble scaling $R_{rms}/R_o \propto \beta \alpha^{1/5}$. The smooth change between these limits indicates a crossover, rather than a transition, between Landau-Pekar and bubble regimes.

Likewise, the relative BEC density change at the impurity position, $|\delta\rho_B(\mathbf{r} = 0)|/\rho$, plotted in Fig. 3 shows the $\sigma^{-1} \propto \alpha^{1/2}$ scaling of the Landau-Pekar polaron on the left side. Before crossing the line of unit relative density response, the curves level off and approach the bubble

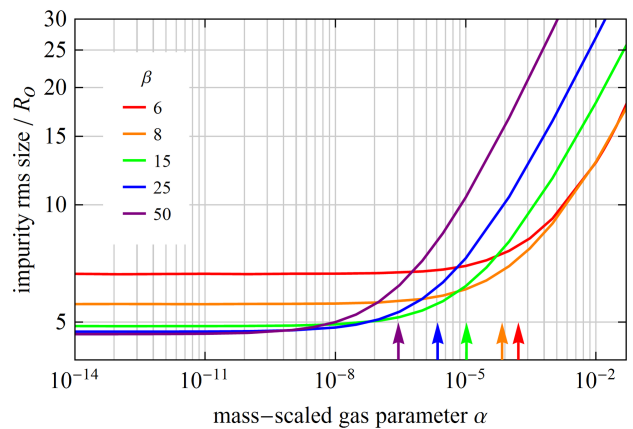


FIG. 2: Dependence on gas parameter α of the r.m.s. width of the impurity density (in units of scaled length R_o), for several values of impurity-BEC interaction parameter β . For each β arrows indicate the values of α for which permeability $\sigma = 1$.

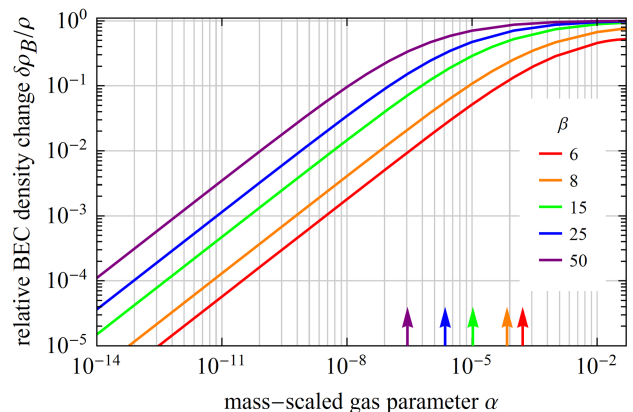


FIG. 3: Dependence on gas parameter α of the relative decrease in BEC density at the impurity location, for several values of impurity-BEC interaction parameter β . For each β arrows indicate the values of α for which permeability $\sigma = 1$.

limit of maximal BEC depletion asymptotically. As in Fig. 2, the arrows on Fig. 3 indicating the $\sigma = 1$ positions illustrate that the crossovers occur near unit permeability. Fig. 4 is the 2D phase diagram for the BEC-impurity system, produced by plotting $|\delta\rho_B(\mathbf{r} = 0)|/\rho$ in the (α, β) -plane, colored to show the polaron regimes and the region where the impurity-BEC interaction is not strong enough to cause self-localization. The red $\sigma = 1$ line lies, as expected, on top of the crossover region.

Experimental realization: The remarkable ability of a BEC to self-localize impurities both in Landau-Pekar and in bubble states could be strikingly illustrated by an experiment that adiabatically Feshbach-tunes the same BEC-impurity system from one limit to the other. For typical densities ($10^{11} \text{ cm}^{-3} < \rho < 10^{14} \text{ cm}^{-3}$) and realistic ranges for a_{BB} and m_B/m_I , we find that cold atom α values may range from 10^{-7} to 10^{-1} . Increasing

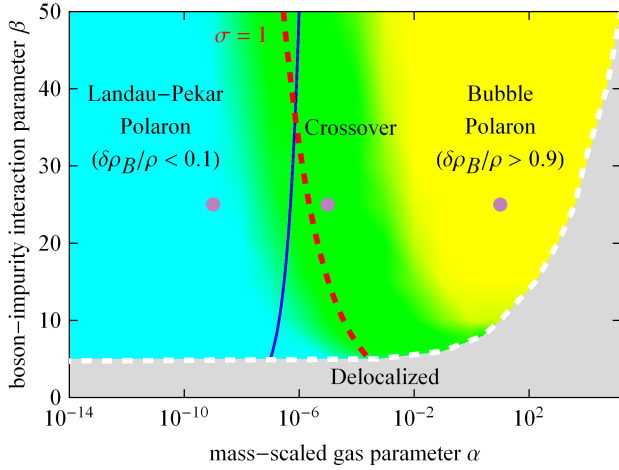


FIG. 4: Phase diagram of the BEC-impurity system obtained as a plot of $|\delta\rho_B(\mathbf{r}=0)|/\rho$. The dots in the Landau-Pekar, crossover, and bubble regions correspond to the BEC density profiles in Fig. 1(a), (b), and (c), respectively. The blue line is a trajectory that tunes the system continuously from Landau-Pekar limit to crossover region to bubble limit (off the top of the plot).

a_{IB} by Feshbach tuning could achieve self-localization at $\beta \sim 5$ (see Fig. 4). Using Eq. (3) and scaling scattering lengths and densities by the typical values of 1 nm and $\bar{\rho} = 10^{13} \text{ cm}^{-3}$, this corresponds to $a_{IB} = a_{IB}^{s.l.}$, where

$$a_{IB}^{s.l.} = \frac{168 \text{ nm}}{\sqrt{\left(1 + \frac{m_B}{m_I}\right) \left(1 + \frac{m_I}{m_B}\right)}} \left(\frac{a_{BB}/\text{nm}}{\rho/\bar{\rho}}\right)^{1/4}. \quad (11)$$

This self-localization near $\beta \sim 5$ results in a Landau-Pekar polaron if $\sigma = [4\pi^{1/4}\sqrt{125\alpha}]^{-1} \gg 1$, requiring

$$a_{BB} \ll 2.00 \text{ nm} (\rho/\bar{\rho})^{-1/3} (m_B/m_I)^{-2/3}. \quad (12)$$

A further increase in a_{IB} and/or ρ can lower the permeability and effect a cross over to the bubble regime when $a_{IB} \sim a_{IB}^{cross}$, where from Eq. (6)

$$a_{IB}^{cross} = 200 \text{ nm} \frac{(\rho/\bar{\rho})^{-1/3} (m_B/m_I)^{-2/3}}{(1 + m_I/m_B)}. \quad (13)$$

Throughout, the permeability parameter varies as

$$\sigma = \frac{1.68}{(a_{IB}/\bar{a}_{IB}^{s.l.})^3} \frac{1}{(\rho/\bar{\rho})^{1/4}} \frac{1}{(a_{BB}/1 \text{ nm})^{3/4}} \left(\frac{m_B}{m_I}\right)^{-\frac{1}{2}}, \quad (14)$$

where $\bar{a}_{IB}^{s.l.}$ denotes the scattering length of Eq.(11) at standard density, $\rho = \bar{\rho}$. The adiabatic (a_{IB}, ρ) variation traces out a trajectory on the phase diagram (e.g. blue line on Fig. 4) that starts in the low α , cyan-colored, Landau-Pekar region. An increase in BEC density (corresponding to an exponential increase in $(\ln \alpha, \beta)$ - space)

and a Feshbach increase in a_{IB} (corresponding to a vertical upward motion in the same space) can then, eventually, steer the BEC-impurity across the green-colored crossover regime into the yellow-colored bubble region.

We now consider two potential issues facing such an experiment. The first is the lifetime of the impurity against three-body recombination. An increase in a_{IB} is generally (but not always – see below) accompanied by a decrease in lifetime [29]. Estimating the three-body limited impurity lifetime τ_I as in [30], we expect $\tau_I^{est} \sim (\sqrt{3}/3.9) \left[\sqrt{1 + 2(m_B/m_I)} (\hbar/m_B) a_{IB}^4 \rho^2\right]^{-1}$. As the time scale of the BEC response (and the slowest time scale in the system), we expect $\tau_B = \hbar/\mu_B$ to set the scale of the self-localization dynamics. The estimated impurity lifetime with full overlap can then significantly exceed τ_B as long as β is not too large,

$$\tau_I^{est} = \tau_B \frac{4\pi^2 \sqrt{3}}{\beta^2 3.9} \frac{(1 + m_I/m_B)^2 (1 + m_B/m_I)^2}{\sqrt{1 + 2m_B/m_I}}. \quad (15)$$

A more careful study of the three-body loss [31] found that τ_I^{est} should be divided by an oscillating Stuckelberg factor related to three-body Efimov physics [32]. Near the nodes of the Stuckelberg factor the lifetime greatly increases. Further, the near complete separation of the impurity and the BEC in the bubble limit implies a significant increase in impurity lifetime for sufficiently large a_{IB} because the three-body recombination loss rate is proportional to the overlap $\int d^3\mathbf{r} \rho_B^2(\mathbf{r}) \rho_I(\mathbf{r})$. We note that in condensed helium, the increased lifetime of positronium [33, 34] has been used as a signal of self-localization [35].

The second challenge faced by an experimental realization of the bubble polaron may be the buoyancy force $\mathbf{F} = -\nabla E_c(\rho) = -(4/5) E_c(\nabla\rho)/\rho$ attempting to expel the impurity from the high density region in an inhomogeneous BEC. A two-color trap or a species specific potential [36, 37] may be necessary to keep the impurity bubble in place. Alternatively, a homogeneous condensate might be created in a flat-bottomed Painted Potential [38]. We note that while the bubble polaron always seeks low BEC density, the Landau-Pekar polaron can be high density seeking.

Conclusion: We have shown that a distinguishable neutral atom embedded in a dilute BEC can, if the BEC-impurity repulsion is strong enough, self-localize in a bubble polaron state in which the impurity is impermeable to the BEC host medium. This state is analogous to that of an electron bubble in condensed helium. Remarkably, and uniquely, the same BEC medium can also self-localize impurities in Landau-Pekar polarons if the BEC density and interaction strengths have appropriate values. We characterized the overlap of the self-localized impurity with the host fluid by a permeability parameter σ that ranges from $\sigma \gg 1$ in the Landau-Pekar limit to $\sigma \ll 1$ in the bubble limit. We have shown that the BEC-impurity system is fully characterized by just two dimensionless coupling constants. In the corresponding

phase diagram, the bubble and Landau-Pekar states correspond to broad regions that are separated by a smooth crossover region near $\sigma \sim 1$. Finally, we pointed out that a single impurity-BEC system can be adiabatically steered from one limit to the other.

E.T. would like to thank the Aspen Center for Physics for a visit, during which part of this work was conceived. This work was partially funded by the Los Alamos National Laboratory LDRD Program.

-
- [1] J. T. Devreese (editor), *Polarons in ionic crystals and polar semiconductors* (North-Holland, Amsterdam, 1972).
- [2] N. N. Bogolubov and N. N. Bogolubov, Jr., *Polaron theory: model problems* (Gordon and Breach, Amsterdam, 2000).
- [3] J. L. Bredas, and G. B. Street, *Acc. Chem. Res.* **18**, 309 (1985).
- [4] E. M. Conwell, *Proc. Natl. Acad. Sci. USA* **102**, 8795 (2005).
- [5] Large polarons have a size that significantly exceeds the lattice constant when the medium is a lattice, in contrast to the lattice polarons discussed in [16–19].
- [6] J. T. Devreese, in *Encyclopedia of Applied Physics*, **14**, 383 (1996).
- [7] J. P. Hernandez, *Rev. Mod. Phys.* **63**, 675 (1991).
- [8] L. D. Landau, *Phys. Z. Sowjetunion* **3**, 644 (1933).
- [9] L. D. Landau, and S. I. Pekar, *J. Exp. Theor. Phys.* **18**, 419 (1948).
- [10] C. G. Kuper, *Phys. Rev.* **122**, 1007 (1961).
- [11] M. H. Anderson, J. R. Ensher, M. R. Matthews, C. E. Wieman, and E. A. Cornell, *Science* **269**, 198 (1995).
- [12] K. B. Davis, M. O. Mewes, M. R. Andrews, N. J. van Druten, D. S. Durfee, D. M. Kurn, and W. Ketterle, *Phys. Rev. Lett.* **75**, 3969 (1995).
- [13] F. M. Cucchietti, and E. Timmermans, *Phys. Rev. Lett.* **96**, 210401 (2006).
- [14] R. M. Kalas, and D. Blume, *Phys. Rev. A* **73**, 043608 (2006).
- [15] Recently, cold atom experiments have realized polarons in a fermion environment: see A. Schirotzek, C.-H. Wu, A. Sommer, and M. W. Zwierlein, *Phys. Rev. Lett.* **102**, 230402 (2009) and C. Kohstall, M. Zaccanti, M. Jag, A. Trenkwalder, P. Massignan, G. M. Bruun, F. Schreck, and R. Grimm, *Nature* **485**, 615 (2012).
- [16] L. Mathey, D. W. Wang, W. Hofstetter, M. D. Lukin, and E. Demler, *Phys. Rev. Lett.* **93**, 120404 (2004).
- [17] M. Bruderer, A. Klein, S. R. Clark, and D. Jaksch, *Phys. Rev. A* **76**, 011605 (2007).
- [18] V. M. Stojanović, T. Shi, C. Bruder, and J. I. Cirac, *Phys. Rev. Lett.* **109**, 250501 (2012).
- [19] A. Mezzacapo, J. Casanova, L. Lamata, and E. Solano, *Phys. Rev. Lett.* **109**, 200501 (2012).
- [20] C. Chin, R. Grimm, P. Julienne, and E. Tiesinga, *Rev. Mod. Phys.* **82**, 1225 (2010).
- [21] Feshbach tuning to $a_{IB} \ll 0$ gives metastable polaron states: see M. Bruderer, W. Bao, and D. Jaksch, *Eur. Phys. Lett.*, **82**, 30004 (2008).
- [22] The true ground state preserves the translational symmetry, but the symmetry breaking energy cost is negligible in the strong-coupling limit.
- [23] N. Bogolubov, *J. Phys. U.S.S.R.* **11**, 23 (1947).
- [24] D. H. Santamore, and E. Timmermans, *New J. Phys.* **13**, 103029 (2011).
- [25] H. Fröhlich, *Adv. Phys.* **3**, 325 (1954).
- [26] W. Casteels, T. Cauteren, J. Tempere, and J. T. Devreese, *Laser Phys.* **21**, 1480 (2011).
- [27] P. Massignan, C. J. Pethick, and H. Smith, *Phys. Rev. A* **71**, 023606 (2005).
- [28] β and σ can also be used as coupling parameters, but we prefer to use α because tuning a_{IB} leaves α unchanged.
- [29] S. Inouye, M. R. Andrews, J. Stenger, H. J. Miesner, D. M. Stamper-Kurn, and W. Ketterle, *Nature* **392**, 151 (1998).
- [30] P. O. Fedichev, M. W. Reynolds, and G. V. Shlyapnikov, *Phys. Rev. Lett.*, **77**, 2921 (1996).
- [31] B. D. Esry, C. H. Greene, and J. P. Burke, *Phys. Rev. Lett.*, **83**, 1751 (1999).
- [32] J. Wang, J. P. D’Incao, B. D. Esry, and C. H. Greene, *Phys. Rev. Lett.*, **108**, 263001 (2012).
- [33] D. A. L. Paul, and R. L. Graham, *Phys. Rev.* **106**, 16 (1957).
- [34] J. Wackerle, and R. Stump, *Phys. Rev.* **106**, 18 (1957).
- [35] R. A. Ferrell, *Phys. Rev.* **108**, 167 (1958).
- [36] J. Catani, G. Barontini, G. Lamporesi, F. Rabatti, G. Thalhammer, F. Minardi, S. Stringari, and M. Inguscio, *Phys. Rev. Lett.* **103**, 140401 (2009).
- [37] G. Lamporesi, J. Catani, G. Barontini, Y. Nishida, M. Inguscio, and F. Minardi, *Phys. Rev. Lett.* **104**, 153202 (2010).
- [38] K. C. Henderson, C. Ryu, C. MacCormick, and M. G. Boshier, *New J. Phys.* **11**, 043030 (2009).